Int. J. Engng Sci. Vol. 29, No. 11, pp. 1357–1362, 1991
Printed in Great Britain.

0020–7225/91 $3.00 + 0.00

SOLUTIONS OF A TWO-DIMENSIONAL DAM BREAK PROBLEM

P. GLAISTER

Department of Mathematics, P.O. Box 220, University of Reading, Whiteknights, Reading RG6 2AX, U.K.

Abstract—Solutions of a two-dimensional dam break problem are presented for two tailwater/reservoir height ratios. The numerical scheme used is an extension of one previously given by the author [*J. Hyd. Res.* **26**(3), 293–306 (1988)], and is based on numerical characteristic decomposition. Thus approximate solutions are obtained via linearised problems, and the method of upwind differencing is used for the resulting scalar problems, together with a flux limiter for obtaining a second order scheme which avoids non-physical, spurious oscillations.

1. INTRODUCTION

The flow of water in a frictionless channel with rectangular cross section and smoothly varying bottom surface is governed by the two-dimensional shallow water equations. The assumptions of hydrostatic pressure distribution and small bottom slope are used in deriving these equations [2]. Since analytical solutions of these equations are not generally available, they are solved numerically.

Several explicit and implicit finite difference methods have been used to solve the shallow water equations [1, 3–7]. One feature of this set of hyperbolic equations is the formation of bores, i.e. discontinuous solutions, which can be difficult to represent accurately even if a shock-capturing method is used. This was found to be the case in [5] where a one-dimensional dam break flow was predicted satisfactorily, although it was found that the speed of the resulting bore was difficult to capture. In [1] a shock-capturing scheme, along the lines of that in [8] for compressible flows of gases, was presented for the one-dimensional shallow water equations, and which overcame these difficulties.

The authors of [5] have recently presented an implicit finite difference scheme [9] capable of treating flows where sub- and super-critical regions are present. They present satisfactory results for a two-dimensional dam break problem, although the bore is still spread over a number of cells. It is this problem that we present solutions for, using an extension of the scheme presented in [1]. The resulting solutions, for two tailwater/reservoir height ratios, show bores captured over two or three cells, but otherwise comparable to those found in [9]. The scheme is also computationally efficient as we demonstrate.

For verification and comparison purposes, we present solutions only to a problem with zero bottom slope and frictionless channel walls. However, the scheme can treat flows where friction terms are included and the bottom slope is non-zero.

2. GOVERNING EQUATIONS

The St. Venant equations governing the flow of water in a channel of rectangular cross section can be written in conservation form as

$$\mathbf{w}_t + \mathbf{F}_x + \mathbf{G}_z = \mathbf{f} + \mathbf{g}, \tag{2.1}$$

where

$$\mathbf{w} = (\phi,\ \phi u,\ \phi w)^T, \tag{2.2a}$$

$$\mathbf{F}(\mathbf{w}) = \left(\phi u,\ \phi u^2 + \frac{\phi^2}{2},\ \phi uw\right)^T \tag{2.2b}$$

$$\mathbf{G}(\mathbf{w}) = \left(\phi w,\ \phi uw,\ \phi w^2 + \frac{\phi^2}{2}\right) \tag{2.2c}$$

$$\mathbf{f}(\mathbf{w}) = (0, g\phi(h_x - s_x), 0)^T \tag{2.3a}$$

$$\mathbf{g}(\mathbf{w}) = (0, 0, g\phi(h_z - s_z)) \tag{2.3b}$$

and

$$\phi = g(\eta + h). \tag{2.4}$$

The quantities $\phi = \phi(x, z, t)$ and $u = u(x, z, t)$ and $w = w(x, z, t)$ represent g multiplied by the total height above the bottom of the channel and the components of the fluid velocity in the x and z directions, respectively, at a general position x, z and at time t. The gravitational constant is represented by g and the undisturbed depth of the water is given by $h(x, z)$. The elevation $\eta = \eta(x, z, t)$ above the plane $y = 0$ is measured in the vertical y direction. The quantitites s_x, s_z are the slopes of the energy grade lines in the x-, z-directions, respectively, and are determined from the steady-state friction formulae (in SI units)

$$s_x = \frac{n^2 u\sqrt{u^2 + w^2}}{(\phi/g)^{4/3}} \tag{2.5a}$$

$$s_z = \frac{n^2 w\sqrt{u^2 + w^2}}{(\phi/g)^{4/3}} \tag{2.5b}$$

where n represents Manning's roughness coefficient. Equation (2.1) has been written so that the right-hand side does not contain any derivatives of flow variables. However, the vectors **f** and **g** are associated with derivatives in the x and z directions, respectively, as a consequence of the terms h_x, s_x and h_z, s_z.

N.B. Equations (2.1)–(2.4), with $s_x = s_z = 0$, represent conservation of mass and momentum. If we combine the mass and momentum equations we arrive at the more familiar equations of motion

$$u_t + uu_x + wu_z = -g\eta_x$$

and

$$w_t + uw_x + ww_z = -g\eta_z.$$

3. OPERATOR SPLITTING

We solve equation (2.1) using an extension of the Riemann solver in [1] together with the technique of operator splitting, [10], i.e. we solve successively

$$\mathbf{w}_t + \mathbf{F}_x = \mathbf{f} \tag{3.1a}$$

and

$$\mathbf{w}_t + \mathbf{G}_z = \mathbf{g} \tag{3.1b}$$

along x- and z-coordinate lines, respectively. We give the scheme for the solution of equation (3.1a) and the scheme for the solution of equation (3.1b) will then follow by symmetry.

4. NUMERICAL SCHEME

Following the approach outlined in [1] for the one-dimensional shallow water equations, a first order, explicit numerical scheme for equation (3.1a) along an x-coordinate line $z = z_0$ can be written as

$$\mathbf{w}_k^{m+1} = \mathbf{w}_k^m - \frac{\Delta t}{\Delta x}\sum_{i=1}^{3} \tilde{\lambda}_i \tilde{\gamma}_i \tilde{\mathbf{e}}_i \tag{4.1}$$

where Δt, Δx represent mesh spacings in the t and x directions, respectively, $\mathbf{w}_k^m$ represents the numerical approximation to the solution $\mathbf{w}(x_j, z_0, m\,\Delta t)$, after m time steps, and at a point x_j on this coordinate line. The value of k could depend on the sign of each $\tilde{\lambda}_i$ (see below) as the technique of upwinding is employed, i.e. k could be j or $j-1$. Thus, the practical implementation of (4.1) is to add

$$-\frac{\Delta t}{\Delta x}\tilde{\lambda}_i\tilde{\gamma}_i\mathbf{e}_i$$

to $\mathbf{w}_{j-1}^m$ if $\tilde{\lambda}_i < 0$ to obtain $\mathbf{w}_{j-1}^{m+1}$, or to add

$$-\frac{\Delta t}{\Delta x}\tilde{\lambda}_i\tilde{\gamma}_i\mathbf{e}_i$$

to $\mathbf{w}_j^m$ if $\tilde{\lambda}_i > 0$ to obtain $\mathbf{w}_j^{m+1}$, for each computational cell (x_{j-1}, x_j) on the coordinate line $z = z_0$. The quantities $\tilde{\lambda}_i$, $\tilde{\mathbf{e}}_i$ represent approximations to the eigenvalues, and eigenvectors, respectively, of the Jacobian $\partial\mathbf{F}/\partial\mathbf{w}$ in the cell (x_{j-1}, x_j). These, together with the appropriate wavestrengths, $\tilde{\gamma}_i$, represent an extension of those contained in [1] for the one-dimensional equations, and a derivation of them can be found in [11]. The required expressions in (4.1) are

$$\tilde{\lambda}_{1,2} = \tilde{u} \pm \tilde{\psi}, \qquad \tilde{\mathbf{e}}_1 = (1,\ \tilde{u} \pm \tilde{\psi},\ \tilde{w})^T, \tag{4.2a, b}$$

$$\tilde{\lambda}_3 = \tilde{u}, \qquad \tilde{\mathbf{e}}_3 = (0,\ 0,\ 1)^T, \tag{4.2c}$$

$$\tilde{\gamma}_{1,2} = \frac{1}{2}\Delta\phi \pm \frac{1}{2}\frac{\tilde{\phi}}{\tilde{\psi}}\Delta u \mp \frac{g\tilde{\phi}(\Delta h - \Delta x\tilde{s}_x)}{2\tilde{\psi}(\tilde{u} \pm \tilde{\psi})} \tag{4.3a, b}$$

$$\tilde{\gamma}_3 = \tilde{\phi}\Delta w \tag{4.3c}$$

$$\tilde{s}_x = \frac{g^{4/3}n^2\tilde{u}\sqrt{\tilde{u}^2 + \tilde{w}^2}}{\tilde{\phi}^{4/3}}, \tag{4.4a}$$

where the approximations to u, w, ϕ and $\sqrt{\phi}$ in (x_{j-1}, x_j) are given by

$$\tilde{A} = \frac{\sqrt{\phi_{j-1}}A_{j-1} + \sqrt{\phi_j}A_j}{\sqrt{\phi_{j-1}} + \sqrt{\phi_j}}, \qquad A = u \text{ or } w, \tag{4.5a, b}$$

$$\tilde{\phi} = \sqrt{\phi_{j-1}\phi_j} \tag{4.5c}$$

and

$$\tilde{\psi} = \sqrt{1/2(\phi_{j-1} + \phi_j)}, \tag{4.5d}$$

respectively. The differences are defined by

$$\Delta A = A(x_j, z_0) - A(x_{j-1}, z_0), \qquad A = \phi, u, w, h. \tag{4.6a–d}$$

The corresponding scheme for equation (3.1b), together with the resulting values of $\tilde{\lambda}_i$, $\tilde{\gamma}_i$ and $\tilde{\mathbf{e}}_i$, can easily be deduced by symmetry.

In summary, we note the direction of flow of information given by the approximate eigenvalues $\tilde{\lambda}_i$ and use this information to update the solution consistent with the theory of characteristics of equation (3.1a). In addition, second order transfers of these first order increments can be made to achieve higher accuracy, providing they are limited to maintain monotonicity [12]. The use of these "flux-limiters" improves accuracy without introducing non-physical spurious oscillations, especially at bores. To allow depression waves to be treated correctly, the first order increment can be considered as two separate increments being sent to either end of the cell [13]. Both these techniques were employed in [1] and will be used to determine numerical solutions of the dam break problem of the next section.

5. RESULTS FOR THE TWO-DIMENSIONAL DAM BREAK PROBLEM

We present results for the two-dimensional dam break problem considered in [9], the details of which we now give.

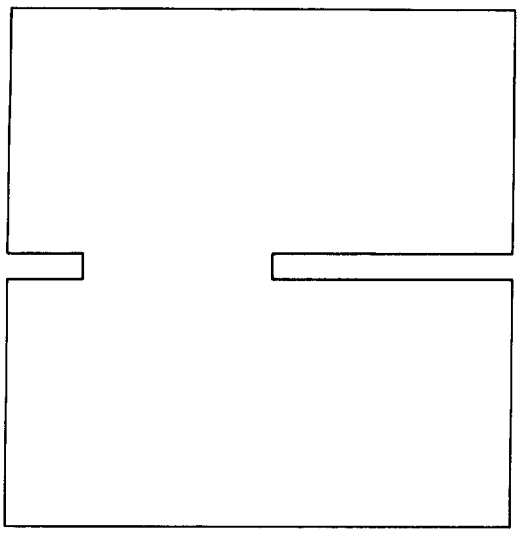

Fig. 1. Computational domain.

The computational domain is defined by a channel 200 m long and 200 m wide. The non-symmetrical breach is 75 m and the dam is 10 m thick, as shown in Fig. 1. The grid is 41×41 points resulting in a mesh size of 5 m by 5 m. For comparison purposes, we present results for a horizontal, frictionless channel. Two initial conditions are chosen, again to coincide with those in [9] and these are

(a) $$\phi_1/g = 10, \qquad \phi_0/g = 5$$

and

(b) $$\phi_1/g = 10, \qquad \phi_0/g = 0.05,$$

representing tailwater/reservoir height ratios of 0.5 and 0.005, respectively (see Fig. 1). We use the scheme described in Section 4 together with the "Minmod" flux-limiter (see [12]).

The results displaying surface elevation contours for these two cases are shown in Figs. 2(a) and 2(b) at time $t = 7.1$ s. (N.B. The figures display contours where the dam is still intact since it is not possible to mask these areas.) In both cases we see that the bore has developed well and has been captured over two or three cells. Only in case (a) is there significant reflection from the wall. This compares favourably with the results found in [9] where the bore is smeared over a number of cells. It is noted by the authors of [9] that many numerical schemes have difficulty in computing accurate solutions, if any, for small ratios of tailwater/reservoir height. We note, however, in computing these satisfactory results we have not expended a great deal of effort in respect of computer time used, or even in storage requirements, merely the use of an efficient, shock-capturing scheme. Using an Amdahl V7 with 41×41 mesh points and the "Minmod" limiter takes 0.3 c.p.u. seconds to compute one time step and a total of 10.5 c.p.u. seconds to reach a real time of 7.1 s using 35 time steps.

The boundary conditions at inflow are prescribed as the initial conditions, whilst on outflow all information is leaving the computational domain and therefore nothing has to be done. At rigid walls we employ the natural extension to the reflecting boundary conditions described in [1]. Thus mesh points, and the resulting cell, straddle a rigid wall boundary, and the surface elevation (and tangential velocity) is prescribed to be the same at each end of such a cell; whereas the normal velocity has the same magnitude, but opposite sign, at each end of such a cell. This enables the boundary conditions to be overwritten along rigid wall boundaries.

6. CONCLUSIONS

A conservative finite difference scheme has been used for the solution of a two-dimensional dam break problem governed by the shallow water equations of ideal fluid flow, and is based

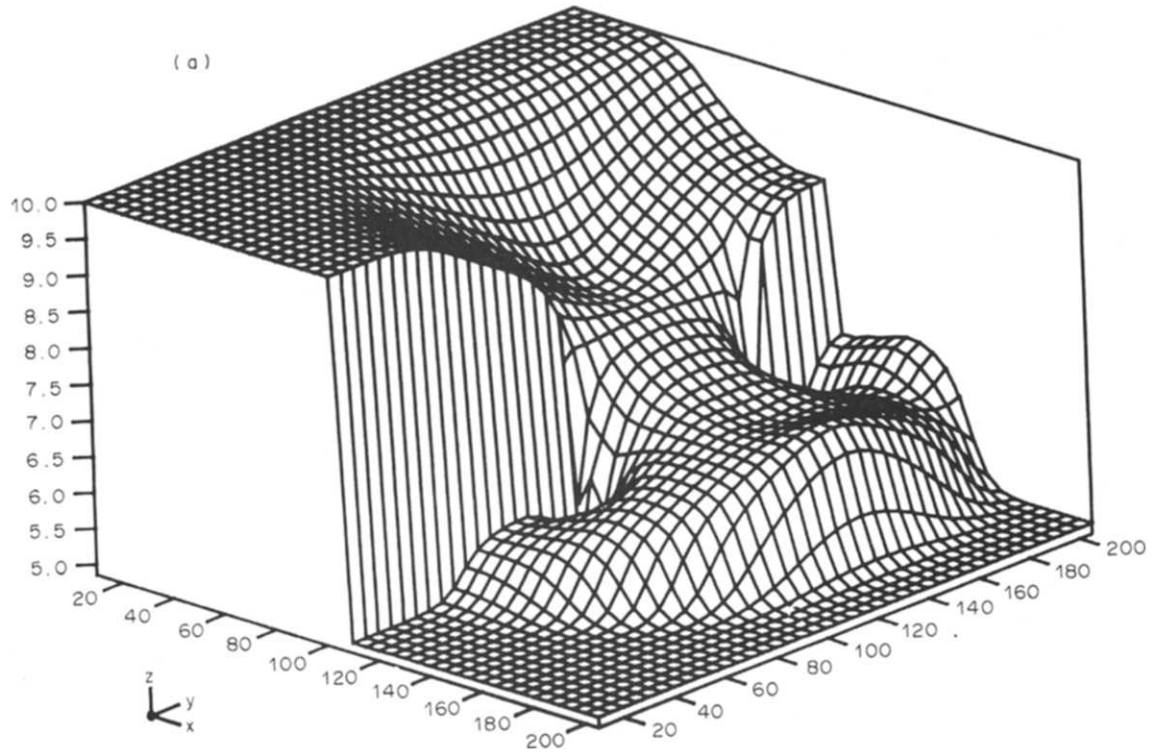

Fig. 2(a). Contours of surface elevation for tailwater/reservoir height ratio 0.5 at time 7.1 s.

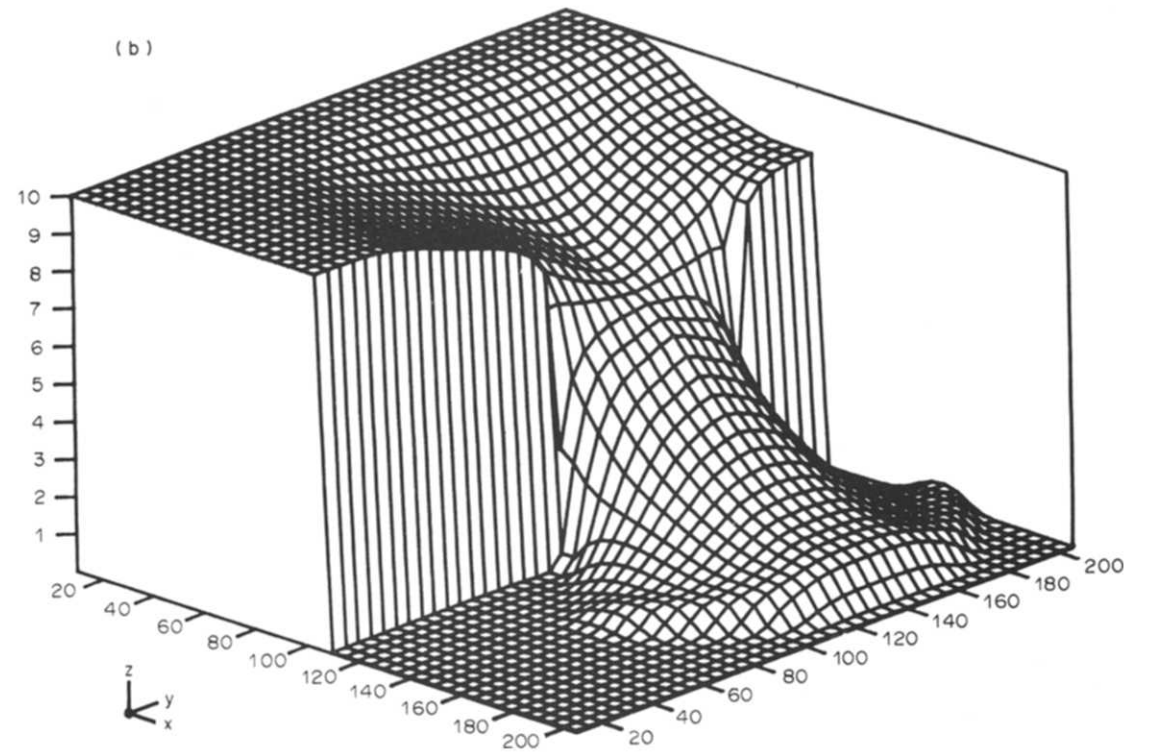

Fig. 2(b). Contours of surface elevation for tailwater/reservoir height ratio 0.005 at time 7.1 s.

on flux difference splitting. The results compare favourably with those produced recently using a different scheme, in particular, the resulting bore is captured over fewer cells. The scheme is also capable of treating flows where friction and bottom slope terms are included.

REFERENCES

[1] P. GLAISTER, *J. Hyd. Res.* **26** (3), 293–306 (1988).
[2] J. J. STOKER, *Water Waves.* Wiley–Interscience, New York (1957).
[3] M. B. ABBOTT, *Computational Hydraulics: Elements of the Theory of Free-Surface Flows.* Pitman, London (1979).
[4] J. CUNGE, F. M. HOLLEY and A. VERWEY, *Practical Aspects of Computational River Hydraulics.* Pitman, London (1980).
[5] R. J. FENNEMA and M. H. CHAUDRY, *J. Hyd. Res.* **25** (1), 41–51 (1987).
[6] J. P. VILA, *SIAM J. Numer. Anal.* **23,** 1173 (1986).
[7] J. P. VILA, Schemas numeriques en hydraulique des ecoulements avec discontinuities. *Proc. XII Congress IAHR,* Lausanne (Edited by J. A. CUNGE and P. ACKERS) (1987).
[8] P. GLAISTER, *J. Comput. Phys.* **74** (2), 382–408 (1987).
[9] R. J. FENNEMA and M. H. CHAUDRY, *J. Hyd. Res.* **27** (3), 321–332 (1989).
[10] N. N. YANENKO *The Method of Fractional Steps.* Springer, Berlin (1971).
[11] P. GLAISTER, Difference schemes for the shallow water equations. Numerical Analysis Report, University of Reading (1987).
[12] P. K. SWEBY, *SIAM J. Numer. Anal.* **21,** 995 (1984).
[13] P. K. SWEBY, A modification of Roe's scheme for entropy satisfying solutions of scalar non-linear conservation laws. Numerical Analysis Report, University of Reading (1982).

(Received 26 November 1990; accepted 22 March 1991)